

Design, syntheses and applications of chemical precursors to advanced ceramic materials in nanostructured forms

Larry G. Sneddon*, Mark J. Pender, Kersten M. Forsthoefel, Upal Kusari, Xiaolan Wei

Department of Chemistry, University of Pennsylvania, Philadelphia, 231 South 34th Street, Philadelphia 19104-6323, PA, USA

Available online 17 September 2004

Abstract

Our recent work directed at the syntheses, characterizations and applications of new organodecaborane molecular and polymeric precursors to technologically important nonoxide ceramic materials, such as boron carbide, is presented. When used in conjunction with currently available methods for nanofabrication, these new precursors enable the formation of ceramic nanostructures, including nanofibers, nanocylinders and nanoporous materials.

© 2004 Elsevier Ltd. All rights reserved.

Keywords: Polymeric organodecaboranes; Nanostructures; Boron carbide

1. Introduction

Boron carbide is a highly refractory material that is of great interest for both its structural and electronic properties.¹ Its chemical inertness, low density (2.52 g/cm³), high thermal stability, hardness, high cross-section for neutron capture, and excellent high-temperature thermoelectric properties give rise to numerous applications, including uses as an abrasive wear-resistant material, ceramic armor, a neutron moderator in nuclear reactors and, potentially, for power generation in deep space flight applications.²

Boron carbide is normally represented by a B₄C (B₁₂C₃) composition with a structure based on B₁₁C icosahedra and C–B–C intericosahedral chains, but single-phase boron carbides are also known with carbon concentrations ranging from 8.8 (~B_{10.5}C) to 20 (~B₄C) at.%. This range of concentrations is made possible by the substitution of boron and carbon atoms for one another within both the icosahedra and the three-atom chains.

While boron carbide powders are easily made by the direct reaction of the elements at high temperatures, new synthetic methods that allow the formation of pure boron carbide in processed forms still need to be developed. We report here

that newly developed molecular and polymeric organodecaboranes are excellent single-source precursors to boron carbide and that these precursors enable the production of nanostructured forms of the ceramic.

2. Experimental details

2.1. Precursor syntheses

The 6,6'-(CH₂)₆-(B₁₀H₁₃)₂ (**1**),³ 6-CH₂=CH(CH₂)₄-B₁₀H₁₃ (**2**),³ [6-(CH₂)₆-B₁₀H₁₃]_x (**3**),⁴ 6-C₇H₉-B₁₀H₁₃ (**4**),⁵ 6-C₈H₁₃-B₁₀H₁₃ (**5**),⁵ [6-C₇H₉-B₁₀H₁₃]_x (**6**),⁵ and [6-C₈H₁₃-B₁₀H₁₃]_x (**7**)⁵ were synthesized as previously described.

2.2. Template synthesis of boron carbide nanocylinders

Following the methods reported by Martin,⁶ alumina membranes (Whatman Anapore filters) having a thickness of 60 μm and a pore size of 200 nm were used as templates. A solution of the precursor (ca. 20 wt.%) was filtered through the membrane via application of vacuum. Once the membrane appeared to be dry on the surface, the coated template was transferred to an alumina boat and then pyrolyzed in

* Corresponding author. Tel.: +1 215 898 8632; fax: +1 215 573 6743.
E-mail address: lsneddon@sas.upenn.edu (L.G. Sneddon).

a tube furnace under a flow of high purity argon to 900 or 1025 °C at 10 °C/min and held at the final temperature for 3 h. After cooling the sample overnight under a constant flow of argon, the alumina template was dissolved by immersing the sample in 48% hydrofluoric acid for 36 h. Isolation of the resulting nanocylinders was achieved by centrifugation of the hydrofluoric acid wash followed by removal of the supernatant fluid and repetitive washing with water, methanol and acetone. Further drying occurred overnight at 80 °C.

2.3. Nanoporous materials

Following the procedure used by Colvin and co-workers,⁷ monodispersed SiO₂ nanospheres with diameters ranging from 200 to 700 nm were produced by TEOS (tetraethyl orthosilicate) hydrolyses in ammonical ethanol. Three-dimensionally ordered planar colloidal silica arrays with thicknesses ranging from one monolayer to 50 μm were then fabricated on quartz microslides by convective self-assembly of the beads during the evaporation of the ethanol solvent. The templated slide was then covered with another microslide with the aid of Teflon spacers. This microslide sandwich was then placed in contact with 6,6'-(CH₂)₆-(B₁₀H₁₃)₂ at 140 °C under nitrogen. The template sandwich was allowed to absorb the precursor by capillary action (~5 min). The flask was then filled with N₂ and the template moved to a tube furnace where it was heated under argon to 1025 °C and held at this temperature for 3–5 h.

One of the template slides was then separated and the microslide with the colloidal crystal material was placed in 48% HF for 10 h. The nanoporous structure separated from the slide during the process.

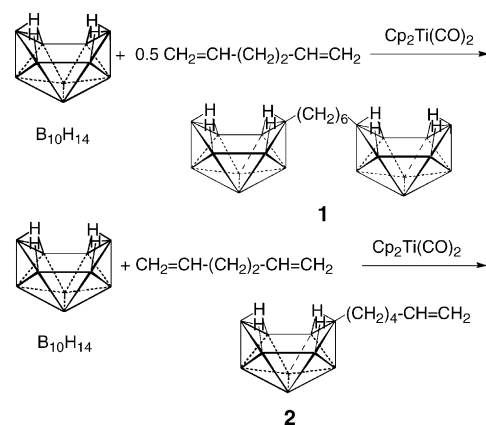
3. Results and discussion

As part of our interest in the design of new polymeric precursors to non-oxide ceramics, we have been investigating the development of new molecular organodecaborane and polymeric poly(organodecaborane) precursors to boron carbide. As described in the following two sections, our recent work has resulted in new metal catalyzed routes to such materials.

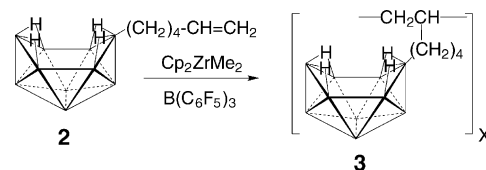
3.1. Early transition metal catalyzed routes to poly(alkenyldecaboranes)

We have reported³ that the titanium catalyzed hydroboration reactions of decaborane with 1,5-hexadiene provides, depending upon the reaction stoichiometry, excellent yields (>88%) of either the linked-cage 6,6'-(CH₂)₆-(B₁₀H₁₃)₂ (**1**) or the hexenyl-substituted derivative 6-CH₂=CH(CH₂)₄-B₁₀H₁₃ (**2**) (Scheme 1).

While it has not been possible to polymerize 6-hexenyldecaborane by employing either thermal or free radical methods, we have found⁴ that it can be readily polymerized by the Cp₂ZrMe₂/B(C₆F₅)₃ catalyst system⁸ to yield a



Scheme 1. Titanium catalyzed syntheses of **1** and **2** from decaborane.



Scheme 2. Dimethylzirconocene catalyzed synthesis of poly(hexenyldecaborane) (**3**).

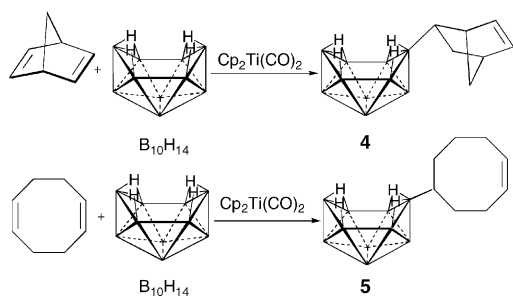
new type of inorganic/organic hybrid polymer composed of a polyolefin backbone with pendant decaboranes (Scheme 2).

In a typical reaction, 1 mol% of the dimethylzirconocene and slightly greater than 1 mol% of the cocatalyst were stirred rapidly at 5–10 °C in minimal benzene with the monomer for 1.5 h. Following reaction termination, the catalyst, monomer and polymer were separated by column chromatography. A 70–75% conversion of monomer to polymer and ~96% isolated yield of polymer were obtained under these conditions. The poly(hexenyldecaborane) (**3**) was isolated as an off-white solid that was soluble in benzene and polar organics with molecular weights (determined by viscometry) of $M_n = 3950$ and $M_w = 5860$ ($M_w/M_n = 1.48$). The spectroscopic data support the structure shown in Scheme 2 consisting of a polyolefin-backbone with pendant decaboranes.

3.2. Ruthenium catalyzed syntheses of poly(organodecaboranes)

We have recently found⁵ that ruthenium-catalyzed ring opening metathesis polymerization (ROMP)⁹ of organodecaboranes containing cyclic-olefin substituents provides a new alternative route to poly(organodecaborane) polymers. As shown in Scheme 3, the high yield syntheses of the key decaboranyl-substituted norbornene and cyclooctene monomers were achieved by employing the titanium-catalyzed reaction of decaborane with norbornadiene and cyclooctadiene, respectively.

Typical conditions employed for the syntheses of these monomers involved the reaction of a large excess of the

Scheme 3. Titanium catalyzed syntheses of **4** and **5** from decaborane.

olefin with decaborane in the presence of ~ 3 mol% catalyst at 90°C for 72 h. The products were easily isolated in excellent yields (**4**: 98% and **5**: 96%) from the metal catalyst by filtration through silica gel. As shown in Fig. 1, a single crystal X-ray structural determination of **4** confirmed a 6-substituted norbornenyl-decaborane structure resulting from the titanium-catalyzed hydroboration of the norbornadiene C5–C6 double bond.

Because of their air stability and tolerance to various functional groups, “Grubbs-type” ROMP catalysts, $\text{Cl}_2(\text{PCy}_3)\text{Ru}(\text{=CHPh})\text{L}$, $\text{L} = \text{PCy}_3$ (**I**) or IMesH_2 (**II**), appeared to be ideal candidates for the syntheses of polyborane polymers. Indeed, ROMP of monomers **4** and **5** with either the first-generation (**I**) or second-generation (**II**) catalyst readily yielded the poly(norbornenyldecaborane) (**6**) and poly(cyclooctenyldecaborane) (**7**) polymers shown in Scheme 4.

Polymerization reactions were carried out at room temperature in a minimum of CH_2Cl_2 solvent using 1 or 2 mol% of the catalyst. Both **I** and **II** catalyzed the polymerization of **5** and **6** to give $\sim 90\%$ conversions in a 1-h reaction time. After reaction termination, the polymers were isolated by column chromatography using pentane and CH_2Cl_2 eluents. Following precipitation in pentane, the polymers were isolated as air stable, white solids that were readily soluble in CH_2Cl_2 and THF. The ^1H and ^{11}B NMR spectra of the polymers show spectral patterns characteristic of a 6-substituted decaborane. Molecular weight studies of **6** and **7** by size exclusion chromatography employing both multi-angle light scattering and differential refractive index (DRI) detectors showed that

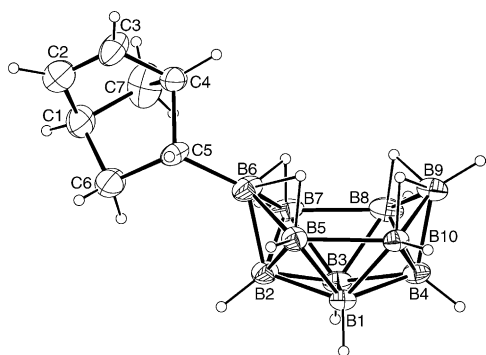
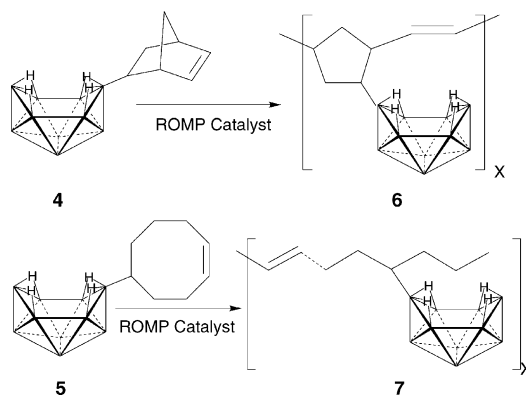


Fig. 1. ORTEP view of the molecular structure of 6-norbornenyldecaborane.

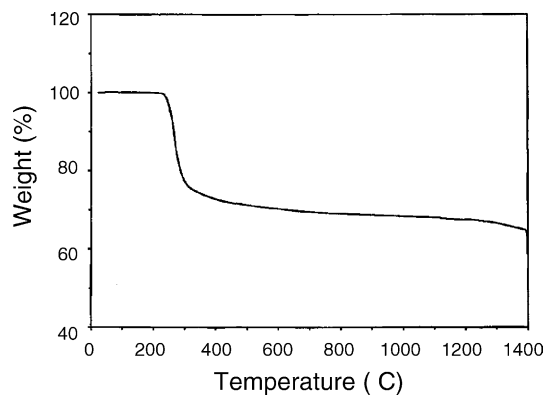
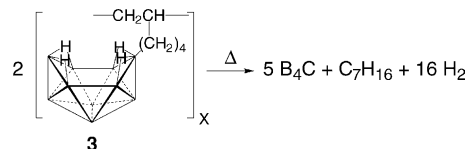
Scheme 4. Ruthenium catalyzed ROMP syntheses of poly(norbornenyldecaborane) (**6**) and poly(cyclooctenyldecaborane) (**7**).

molecular weights with M_n in excess of 30 kDa and polydispersities between 1.1 and 1.8 can be readily obtained.

3.3. Ceramic conversion studies

The poly(hexenyldecaborane) T_g 's are in the $50\text{--}60^\circ\text{C}$ range and the TGA study in Fig. 2 showed that polymer decomposition does not begin until $\sim 225^\circ\text{C}$. Thus, these polymers are stable as melts. According to the TGA, the ceramic conversion reaction is essentially complete by 600°C . The observed TGA (65%) and bulk (60%) ceramic yields are close to the theoretical ceramic yield of 68% (Scheme 5).

As presented in Fig. 3, XRD studies of the black, glassy ceramics obtained upon bulk pyrolyses of the polymer showed that samples heated to only 1000°C were amorphous, but those heated at 1250°C (1 h) exhibited the onset of boron

Fig. 2. Thermogravimetric analysis (TGA) study of poly(hexenyldecaborane) (**3**).Scheme 5. Ceramic conversion reaction of **3** to boron carbide.

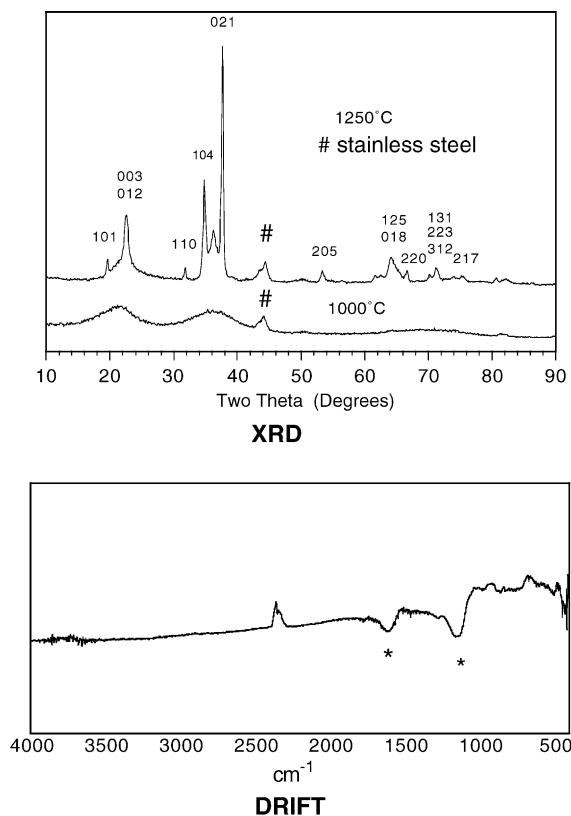


Fig. 3. X-ray diffraction (XRD) and diffuse reflectance infrared (DRIFT) studies of ceramics derived from poly(hexenyldecaborane) (3).

carbide crystallization. Highly crystalline materials were obtained by heating the ceramics to 1850 °C. The diffuse reflectance infrared (DRIFT) spectrum (Fig. 3) of a sample heated at 1250 °C (1 h) showed the characteristic boron carbide bands at 1605 and 1144 cm^{-1} .¹⁰

Elemental analyses of the resulting boron carbide ceramics derived from poly(hexenyldecaborane) indicate compositions in the range of B_4C . As discussed earlier, boron carbide can have a range of compositions ranging from 8.8 to 20 at.% carbon and the ceramics derived from the poly(hexenyldecaborane) are thus on the “carbon-rich” side.

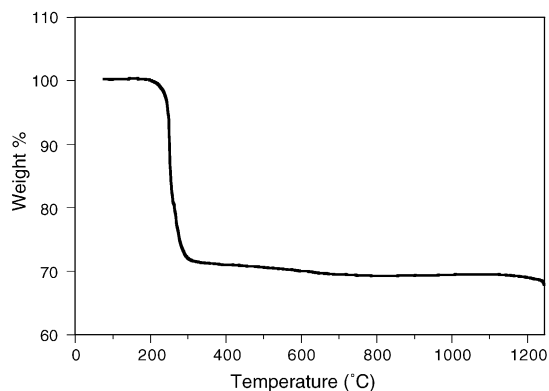


Fig. 4. TGA study of 6,6'-(CH_2)₆-($\text{B}_{10}\text{H}_{13}$)₂ (2).

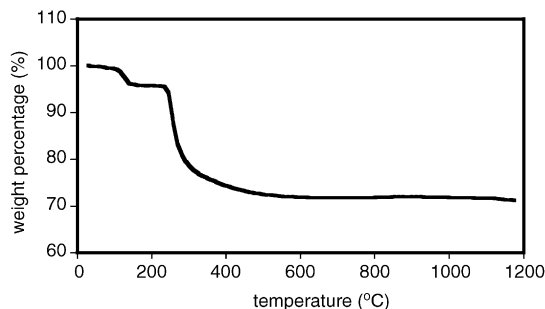


Fig. 5. TGA study of poly(norbornenyldecaborane) (6).

The TGA study in Fig. 4 of the 6,6'-(CH_2)₆-($\text{B}_{10}\text{H}_{13}$)₂ ceramic-conversion reaction showed that decomposition begins near 220 °C and is essentially complete by 400 °C.

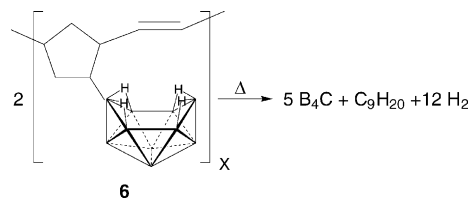
The XRD analyses of bulk powder samples of 6,6'-(CH_2)₆-($\text{B}_{10}\text{H}_{13}$)₂ pyrolyzed at 1000 °C (3 h) indicated that they were amorphous, but powders heated at 1025 °C (3 h) exhibited the characteristic boron carbide diffraction pattern. Likewise, DRIFT spectra of powders heated at 1025 °C (3 h) showed the major boron carbide bands.

Since the boron to carbon ratio (20:6) in 6,6'-(CH_2)₆-($\text{B}_{10}\text{H}_{13}$)₂ is much higher than that in the poly(hexenyldecaborane) (10:6), it was expected to provide access to “boron-rich” boron carbide compositions and, indeed, elemental analyses of the 1000 °C (B, 88.4%; C, 11.5%) and 1025 °C (B, 89.0; C, 10.8%) pyrolyzed powders showed no measurable hydrogen and established $\text{B}_{7.7}\text{C}$ and $\text{B}_{8.3}\text{C}$ compositions, respectively.

A TGA study (Fig. 5) of the ceramic conversion reaction (Scheme 6) of the ROMP-synthesized polymer 6 indicated that weight loss begins near 100 °C and is essentially complete by 500 °C to give a final char yield of 72%. Elemental analysis of a 1650 °C char (B, 67.9%; C, 32.2%) corresponded to a $(\text{B}_4\text{C})_{1.0}(\text{C})_{0.75}$ composition. XRD analyses indicated that chars up to 1200 °C were amorphous, but, while still retaining a substantial amorphous component, those samples pyrolyzed at 1300 and 1650 °C showed the characteristic boron carbide peaks along with graphite peaks at 26 and 42 2-theta. The excess carbon in these chars undoubtedly retards boron carbide crystallization.

3.4. Nanostructured ceramics

The polymer precursor route to ceramics has been widely used to produce micron scale materials,¹¹ but new technologies are demanding smaller sizes. Nanoscale ceramic



Scheme 6. Ceramic conversion reaction of 6 to boron carbide.

materials are of particular interest due to their potential applications in electronic and optical devices, structural reinforcements, catalyst supports and membranes for gas separations.¹²

3.4.1. Nanofibrous and nano-cylindrical boron carbide structures

Owing to their small size, the traditional fiber spinning techniques that are used to produce micron scale fibers are inapplicable for the production of nanofibers. However, new porous alumina templating methods have recently been widely used to generate nanofibers from a variety of materials including polymers, carbon, metals, semiconductors and ceramics.⁶ This template method involves the absorption of a precursor material into the channels of the nanoporous alumina using either gas-phase or solution methods, conversion of the precursors to the final solid state material by thermolytic or chemical reactions, and then dissolution of the alumina membrane to leave the free standing fibers. In our work, we used alumina membranes having a thickness of 60 μm and a nominal pore size of ~ 250 (± 50) nm. Boron carbide nanofibers were generated¹³ by initially filling the membranes with liquid 6,6'-(CH_2)₆-($\text{B}_{10}\text{H}_{13}$)₂ at 140 °C, then pyrolyzing the filled templates at 1025 °C (1 h) to produce a boron carbide filled membrane. Immersing the sample in 48% hydrofluoric acid for 36 h dissolved the alumina template. The scanning electron microscopy (SEM) image in Fig. 6 shows a sample of nanofibers prepared as described above. The fibers are uniform with an ~ 250 nm diameter and ~ 45 μm length. X-ray diffraction studies of these fibers showed that while the 1000 °C fibers are largely amorphous, the 1025 °C fibers are composed of crystalline boron carbide. A thin layer of boron carbide was allowed to remain on one end of the fibers. This layer serves to hold the fibers in their parallel arrangement giving the highly aligned, brush-like configuration that is apparent in Fig. 6. As has been previously noted, one of the advantages of the templating technique over other methods for generating nanofibers is its natural ability to produce aligned, monodispersed ensembles of nanofibers.

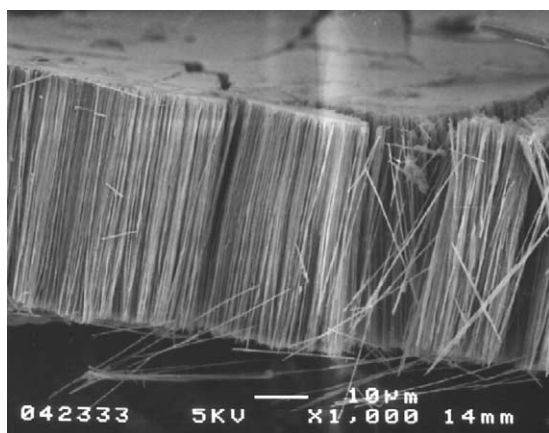


Fig. 6. SEM image of the boron carbide nanofibers.

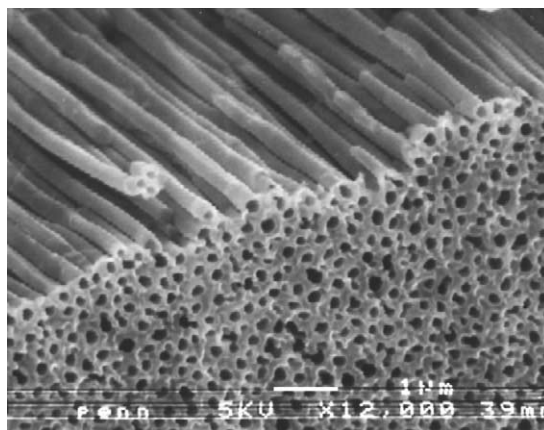


Fig. 7. SEM image of an end view of the boron carbide nanocylinders.

We have now also found that ceramic nanocylinders can be generated by a procedure similar to that reported by Martin and co-workers^{6(a,j)} for the production of polymer nanotubes. Such hollow fiber structures are of great potential importance, since they could prove useful for the construction of multi-component nanofibers. In order to avoid completely filling the channels of the porous alumina, the template is either only briefly dipped in the neat precursor or is treated with a precursor solution. In the latter process, a toluene solution of the poly(hexenyldecaborane) precursor was vacuum filtered through the template. The solvent was then completely evaporated to leave a thin precursor layer on the surfaces of the membrane. Pyrolysis of the coated membrane converted the precursor to a boron carbide coating.

Dissolution of the coated alumina membranes with HF then yielded free-standing nanocylindrical boron carbide structures. The SEM image in Fig. 7 shows a side view of an ensemble of boron carbide nanocylinders that are ~ 50 μm long and ~ 250 nm in diameter and clearly shows the hollow cores of the cylindrical structures. The inside diameter and wall thickness of the nanocylinders can be controlled by the solution concentration and/or number of membrane treatments.

In our initial studies of the syntheses of both nanofibers and nanocylinders, we have employed ~ 250 nm templates, but nanoporous alumina templates have been prepared with channels as small as 5 nm. We are now applying the methods that we developed in our initial work to generate and study these smaller dimension boron carbide (as well as other nonoxide ceramic) fibers and nanocylinders.

3.4.2. Nanoporous boron carbide structures

The design of solids with ordered macroporosities has recently received great attention because of the possibility that such materials could serve as photonic bandgap and optical stop-gap materials, as well as catalyst supports and gas separation membranes.¹⁴ Although methods for producing ordered porous materials with pore diameters less than 10 nm are well developed, only recently have techniques

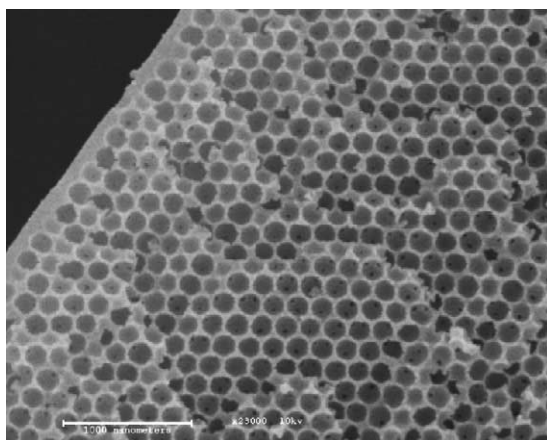


Fig. 8. SEM image of a nanoporous boron carbide array.

for producing uniform macroporous (>25 nm) materials been reported.^{7,14} These methods generally involve the controlled growth of a matrix around an ordered array of macroscale templates. Silica spheres, latex beads and triblock copolymers have each been employed as templates. Once the matrix structure is formed, the templates are then removed, by either chemical etching or thermal decomposition, to leave a macroporously ordered inorganic solid. For example, latex beads have been used as templates to construct, via sol-gel condensations, ordered macroporous arrays of titania, zirconia, and alumina. Other work employing the silica templates have yielded macroporous carbons.

We have now used this templating technique to make macroporous nonoxide ceramic structures. Our initial studies have focused on the generation of macroporous boron carbide structures using the 6,6'-(CH₂)₆-(B₁₀H₁₃)₂ molecular precursor.

A macro-ordered silica array was first generated by employing the method recently reported by Colvin and co-workers.⁷ Following the procedure outlined in the experimental section, the open space in this framework was then filled with the boron-carbide precursor 6,6'-(CH₂)₆-(B₁₀H₁₃)₂ by immersion in a melt of the compound. Pyrolysis of the filled body to 1025 °C, then yielded a boron carbide matrix surrounding the silica spheres. The silica spheres were then etched from the matrix by treatment with 48% HF to leave a “holey” boron-carbide framework.

The SEM image in Fig. 8 indicates a boron carbide framework with reasonably ordered ~50 nm pores. We are now optimizing our procedures to both increase the ordering of the framework and achieve control of the hole size (through the use of different size silica beads) of the boron carbide framework.

4. Conclusions

Organodecaborane materials appear to be ideal precursors for the synthesis of boron carbide materials in processed

forms: (1) they are readily synthesized in large amounts using metal catalyzed reactions; (2) they contain no other ceramic forming elements and can be designed to yield “carbon-rich” (~B₄C) or “boron-rich” (~B₈C) boron carbide compositions; (3) they are stable as melts, thus allowing the use of melt-processing methods; and (4) upon pyrolysis, they undergo crosslinking reactions at relatively low temperatures (~220 °C) which retards loss of material by volatilization, thereby generating high ceramic and chemical yields. The use of designed molecular and polymeric precursors in conjunction with nano-templating methods allows the systematic generation of a range of nanostructured materials, including nanofibers, nanocylinders and nanoporous ceramics that have been unattainable using traditional synthetic methods. We are now investigating the structural and electronic properties of these materials, as well as the use of these template methods for the production of a wide range of other nanostructured ceramics.

Acknowledgements

We thank the US Department of Energy, Office of Basic Energy Sciences, the Air Force Office of Scientific Research and the National Science Foundation for the support of this project.

References

- (a) Thevenot, F., *Key Eng. Mater.*, 1991, **56/57**, 59;
(b) *AIP Conf. Proc.* 140, ed. D. Emin, T. Aselage, C. L. Beckel, I. A. Howard and C. Wood. Am. Inst. Phys., New York, 1986;
(c) *AIP Conf. Proc.* 231, ed. D. Emin, T. Aselage, A. C. Switendick, B. Morosin and C. L. Beckel. Am. Inst. Phys., New York, 1991.
- (a) Wood, C., In *AIP Conf. Proc.* 140, ed. D. Emin, T. Aselage, C. L. Beckel, I. A. Howard and C. Wood. Am. Inst. Phys., New York, 1986, p. 362 and references therein;
(b) Aselage, T. L., Tallant, D. R., Gieske, J. H., Van Deusen, S. B. and Tissot, R. G., *Phys. Chem. Carbides Nitrides Borides*, 1990, **97**, 12.
- Pender, M. J., Carroll, P. J. and Sneddon, L. G., *J. Am. Chem. Soc.*, 2001, **123**, 12222.
- Pender, M. J. and Sneddon, L. G., *Polym. Prep. (Am. Chem. Soc., Div. Polym. Chem.)*, 2000, **41**, 551.
- Wei, X., Carroll, P. J. and Sneddon, L. G., *Organometallics*, 2004, **23**, 163.
- (a) Martin, C. R., *Science*, 1994, **266**, 1961;
(b) Martin, C. R., *Acc. Chem. Res.*, 1995, **28**, 61;
(c) Martin, C. R., *Chem. Mater.*, 1996, **8**, 1739;
(d) Lakshmi, B. B., Patrissi, C. J. and Martin, C. R., *Chem. Mater.*, 1997, **9**, 2544;
(e) Cepak, V. M., Hulteen, J. C., Che, G., Jirage, K. B., Lakshmi, B. B., Fisher, E. R. and Martin, C. R., *Chem. Mater.*, 1997, **9**, 1065;
(f) Che, G., Lakshmi, B. B., Martin, C. R., Fisher, E. R. and Ruoff, R. S., *Chem. Mater.*, 1998, **10**, 260;
(g) Klein, J. D., Herrick, I. I., Robert, D., Palmer, D. and Sailor, M. J., *Chem. Mater.*, 1993, **5**, 902;
(h) Zelenski, C. M. and Dorhout, P. K., *J. Am. Chem. Soc.*, 1998, **120**, 734;

- (i) Zhang, Z., Gekhtman, D., Dresselhaus, M. S. and Ying, J., *Chem. Mater.*, 1999, **11**, 1659;
- (j) Cepak, V. M. and Martin, C. R., *Chem. Mater.*, 1999, **11**, 1363.
7. (a) Turner, M. E., Trentler, T. J. and Colvin, V. L., *Adv. Mater.*, 2001, **13**, 180;
- (b) Jiang, P., Bertone, J. F., Hwang, K. S. and Colvin, V. L., *Chem. Mater.*, 1999, **11**, 2132;
- (c) Jiang, P., Hwang, K. S., Mittleman, D. M., Bertone, J. F. and Colvin, V. L., *J. Am. Chem. Soc.*, 1999, **121**, 11630;
- (d) Stoeber, W., Fink, A. and Bohn, E., *J. Coll. Interf. Sci.*, 1968, **26**, 62.
8. Yang, X., Stern, C. L. and Marks, T. J., *J. Am. Chem. Soc.*, 1994, **116**, 10015.
9. For some reviews on metal-catalyzed ROMP reactions, see:;
- (a) Grubbs, R. H. and Tumas, W., *Science*, 1989, **243**, 907;
- (b) Schrock, R. R., *Acc. Chem. Res.*, 1990, **23**, 158;
- (c) Buchmeiser, M. R., *Chem. Rev.*, 2000, **100**, 1565;
- (d) Trnka, T. M. and Grubbs, R. H., *Acc. Chem. Res.*, 2001, **34**, 18.
10. Becher, V. H. J. and Thévenot, F. Z., *Inorg. Allg. Chem.*, 1974, **410**, 274.
11. For reviews of ceramic precursors see: *Precursor-Derived Ceramics*, ed. J. Bill, F. Wakai and F. Aldinger. Wiley-VCH, Weinham, 1999 and references therein.
12. Nanoscale Science, Engineering and Technology, Research Directions Report of the Basic Energy Sciences Nanoscience/Nanotechnology Group, US Department of Energy, and references therein (1999).
13. Pender, M. J. and Sneddon, L. G., *Chem. Mater.*, 2000, **12**, 280.
14. *Mater. Res. Soc. Bull.*, 2001, **26**, 608.